Arab J Geosci
DOI 10.1007/s12517-013-0949-7

ORIGINAL PAPER

Solute transport as affected by surface land characteristics in gravely calcareous arid soils

M. Al-Qinna · M. Salahat · K. Mashal

Received: 14 February 2013 / Accepted: 1 April 2013

Abstract Gravely calcareous soils cover approximately most of arid lands (in percent); however, the solute transport behavior in these soils remains a current issue. This research aimed at estimating and correlating the solute transport parameters in gravely calcareous soils as being affected by different land uses through the knowledge of the soil morphological, physical, and chemical properties. Four different land use sites were selected: irrigated trees and bare, range, and alluvial sediment lands. Solute transport parameters of soil pore water velocity (*V*), dispersion coefficient (*D*), and retardation factor (*R*) were estimated using bromide breakthrough curve tests for surface soil columns. In addition, field Brilliant Blue FCF dye tracing experiment was conducted to determine the maximum dimensional movements. Soil morphological analysis was able to explain the heterogeneity in the solute transport parameters. Conductive solute transport mechanism with *V* of 17.99 m/day was favored in a high continuous pore system observed under tree lands. Presence of high gravel and $CaCO_3$ contents under range lands increased pore system tortuosity and thus increased *D* magnitude up to 1,339.88 cm^2/day. Existence of thin surface crusts at both bare soils and alluvial sediments had considerably restricted *V* down to 1.46 m/day. Dye staining technique aided the explanation of the existing variations by providing visual evidence on the preferential flow paths and patterns governing the solute transport mechanism at each site.

M. Al-Qinna · M. Salahat · K. Mashal
Department of Land Management and Environment,
Faculty of Natural Resources and Environment,
Hashemite University, Zarqa, Jordan

M. Al-Qinna (✉)
PO Box 33205, 13133 Amman, Jordan
e-mail: qinna@hu.edu.jo

Keywords Solute transport · BTC · Dye tracing · Soil morphology · Gravel content · Calcareous soils

Introduction

Great efforts have been made to understand the mechanisms of water and solute transport through the vadose zone. The migration of anthropogenic toxic elements due to agricultural practices, transportation, application of sewage sludge, and seepage from landfills have been widely recognized. In order to estimate the magnitude of the hazard caused by these chemicals, it is necessary to understand the processes controlling their movement from the soil surface down to groundwater (Costa and Prunty 2006; Jalali and Moharrami 2007; Samsoe-Petersen et al. 2002).

Accurate mathematical analyses of solute transport in heterogeneous media are not easily achieved (Leij and van Genuchten 1995). Solute transport in soils has traditionally been described with the convection–dispersion equation (CDE) by incorporating two constitutive transport mechanisms: (1) movement as a result of transport of the fluid and (2) spreading as a result of known and unknown processes such as diffusion (Eq. 1).

$$R\theta \frac{\partial C}{\partial t} = D\frac{\partial^2 C}{\partial z^2} - v\frac{\partial C}{\partial z} \quad (1)$$

where *R* is the dimensionless retardation factor [$R=1+(\rho_b K/\theta)(dS/dt)$], ρ_b is the soil bulk density (in kilogram per cubic meter), *K* is the water hydraulic conductivity (in meter per second), *S* is the sorption of solute on solid phase, *D* is the hydrodynamic dispersion coefficient (in square meter per second), θ is the volumetric water content (in cubic meter per cubic meter), *C* is either the flux or resident concentration (in mole per cubic meter), *z* is depth (in meter), and *v* is the pore water velocity (in meter per

Published online: 13 April 2013

second), given by q/θ, where q is the water flux density (in meter per second).

The CDE has been widely used in many researches using breakthrough curve (BTC) analysis in either laboratorial soil columns or at field (Larsbo and Jarvis 2005; Li and Hong 2009; Mojid and Vereecken 2005; Yolcubal and Akyol 2008). There are three main types of boundary conditions: (1) Dirichlet which assumes a constant concentration maintained at one or both ends of the soil, (2) Neuman which implies a specific constant flux density at the surface, and (3) Cauchy by which both the contaminant concentration and its gradient are coupled together as a boundary condition. Van Genuchten and Alves (1982) had provided analytical solutions for a one-dimensional convective–dispersive solute transport equation with varying boundary conditions.

Solute transport in porous systems is greatly affected by properties of the contaminant, soil, as well as the aquifer, climatological factors, and land use/land cover (LULC) patterns (Dousset et al. 2007; Finke and Hutson 2008; Jalali and Moharrami 2007). Soil structure determines to a large extent the solute transport mechanism through the arrangement and distribution of pore system (Ersahin et al. 2002; Jørgensen et al. 2004; Scott 2000; Vogeler et al. 2006). Presence of coarse fragments may influence soil hydraulic properties thus influencing the convective dispersive flow (Al-Qinna et al. 2008).

The lack of knowledge of solute behavior in gravely calcareous arid soils justifies this research. The main objectives of this study are (1) to estimate the solute transport parameters in calcareous soils associated with high gravel content using BTC analyses, (2) compare and correlate between field soil morphology, LULC, and solute transport parameters, and (3) provide further visualization evidence of the solute flow paths in soil pedon using dye tracing technique.

Materials and methods

Site selection and characterization

The study area represents a typical eastern Jordanian arid zone at the desert boundary, with mean annual rainfall of 150 mm and thermic temperature regime. According to the national soil map of Jordan (Ministry of Agriculture 1994), two main soil series are existing at the study area: Xerochreptic Calciorthids and Xerochreptic Cambiorthids (Fig. 1).

Four different sites with varying land cover were selected for this study: soil with irrigated olives trees (T), bare soil (B), range land with native shrubs (R), and stream land associated with alluvial sediments (A). Undisturbed and disturbed soil samples were taken from the four soil sites using a soil core sampler (6 mm in diameter) and environmental auger (6 mm in diameter), respectively. Disturbed soil samples were dried at 105 °C for 24 h, grounded, then sieved through a 2-mm sieve. Gravel content (>2 mm in diameter) was measured by weight method (Grossman and Reinsch 2002).

Five replicates of surface undisturbed samples taken to 10 cm depth were used to determine the bulk density (ρ_b) by coring technique (Blake and Hartge 1986). The disturbed samples were used to estimate total organic carbon by the Walkley–Black wet combustion method (Nelson and

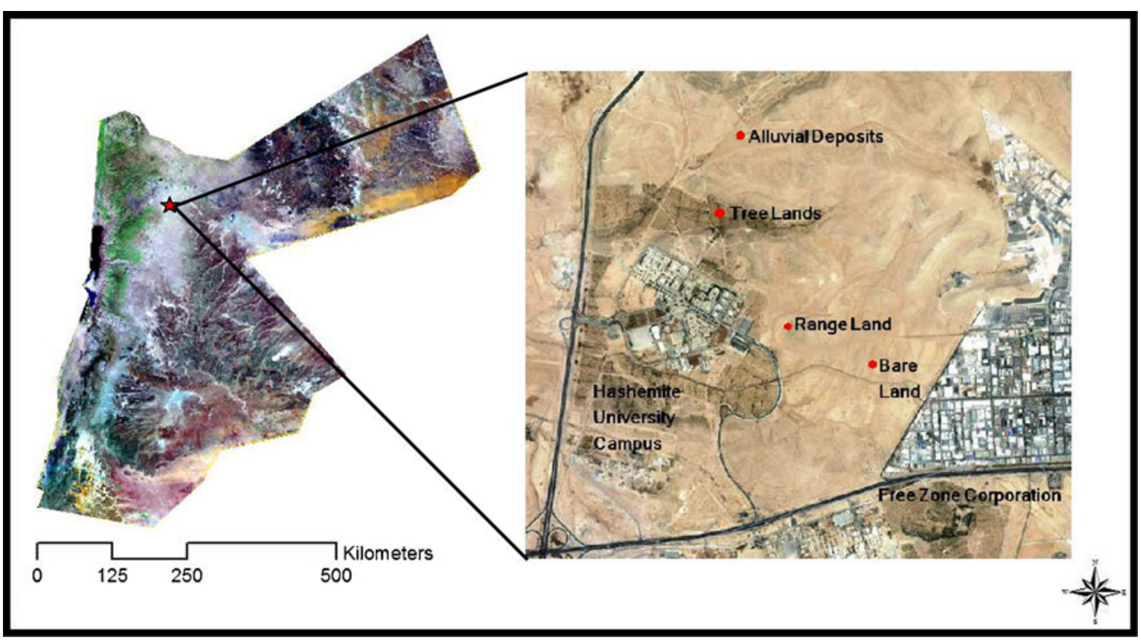

Fig. 1 Location map of the study area showing the four selected sites

Sommers 1996), total soil carbonates using the calcimeter method (Loeppert and Suarez 1996), and particle size distribution using the pipette method (Gee and Bauder 1986). Soil extracts were used to estimate alkalinity (pH) and Electrical Conductivity (ECe) using pH and electrical conductivity (EC) meters (Thomas 1996; Rhoades 1996). Saturated hydraulic conductivities (K_{sat}) were determined using the constant head method (Klute and Dirksen 1986).

In addition, the associated soils of the four land sites were morphologically investigated in situ. Morphological analyses included description of soil structure in terms of pedality. Soil pedons were classified according to size, shape, and grade, while the visible pore systems (larger than 0.05 mm in diameter) were classified in terms of abundance, shape, and continuity.

Breakthrough curve analyses

Three replicates of undisturbed vertical soil columns were collected from each of the four sites at depths of 0 to 10 cm. The cylindrical soil columns were isolated using plexiglass with cutting edge by which excess soil material at the bottom of the cylinders was trimmed flush and caps were secured to the ends to permit transport to the laboratory. Soil columns were mounted vertically, and the columns were initially saturated with 5 mM $CaCl_2$ using a Marriott bottle apparatus adjusted with a stopcock to maintain a constant 5-cm head at the soil surface. The displacement experiments were conducted at saturated condition using 10 mM KBr as the influent solution. The bromide tracer was injected continuously creating a Dirichlet boundary condition maintained on the top of the soil column only after a steady state flux of $CaCl_2$ had been established. A fraction collector was used to collect effluents in a small volume fraction (Klute 1986).

The solution for the bromide concentration (C) at a depth (z) and time (t) with the Dirichlet boundary condition maintained on the top of the soil column is given by Eq. 2 (van Genuchten and Alves 1982).

$$\left.\begin{array}{l} C_l(0,t)=C_0 \\ \frac{dC_l}{dz}(\infty,t)=0 \end{array}\right\}\text{Dirichlet boundary condition}$$

$$C(z,t)=\frac{1}{2}\operatorname{erfc}\left(\frac{Rz-vt}{2\sqrt{DRt}}\right)+\sqrt{\frac{v^2t}{\pi RD}}\times\exp\left(-\frac{(Rz-vt)^2}{4DRt}\right) - \frac{1}{2}\left(1+\frac{vz}{D}+\frac{v^2t}{RD}\right)\times\exp\left(\frac{vz}{D}\right)\times\operatorname{erfc}\left(\frac{Rz+vt}{2\sqrt{DRt}}\right) \quad (2)$$

Bromide concentrations in the effluent solution were measured using ion chromatography (Dionex, Sunnyvale, CA). In addition, thymol was used as a biological inhibitor to stop the biological activity during the experiment. The convective–dispersive equation (van Genuchten and Alves 1982) was fitted to dimensionless effluent concentrations using nonlinear least-squares parameter optimization method using the JMP 8.0 statistical program (JMP 2009). Pore water velocity, soil retardation, and dispersion coefficients were estimated for each site along with indicative statistical capacity of the fitted model designated by root mean square error (RMSE).

Correlation analysis of solute transport parameters with soil properties

For even further explanations, it is useful to identify the strength of the relationships between the soil physical and chemical properties and the solute transport parameters; thus, a correlation matrix was achieved indicating Pearson's product moment correlation coefficient (r). For the purpose of this study, the strength of the correlation was classified into three levels: weak correlation when $0\leq|r|<0.3$, moderate correlation when $0.3\leq|r|<0.7$, and strong correlation when $0.7\leq|r|\leq1.0$ (Wong and Lee 2005). The correlation analyses were performed using multivariate platform within the JMP 8.0 statistical program (JMP 2009).

Dye tracing

The dye tracing study was carried out in the field during the dry season to investigate the dispersion and convection movement in addition to examining macropore flow existence. At every site, a single ring apparatus (30 cm × 30 cm) was inserted into the soil down to 15 cm. In order to have a constant surface wetted area, the confined soil volume within the ring was saturated for 24 h. Two liters of Brilliant Blue FCF (C.I. 42090) dye tracer with a concentration of 10 mg L^{-1} was continuously applied into the ring to produce a cumulative flow pattern of the infiltrating dye in the soil beneath (Ghodrati and Jury 1990; Flury et al. 1994). After the completions of the experiment, the soils under the rings were excavated to the extent of maximum dye lateral and vertical movement.

Results and discussion

Soil characteristics

Generally, the area is characterized by loam soil surface texture (except for the alluvial sediments were it is more of clay loam with clay content of 39.7 %). For Cambiorthid soils, sand and silt percentages exceeded 90 % and clay content ranged from 7.1 to 16.3 %. Gravel content varied considerably in the study sites and ranged from 2 to 30.3 % for bare land and range land, respectively. Also, the study area is characterized by being calcareous and having tremendous dissected rock fragments in gravel size developed from limestone parent material with $CaCO_3$ content that ranged between 32.9 and 52.3 % for bare land and range land, respectively. In addition to the above, both bare land

Table 1 Soil surface morphological, physical, and chemical characteristics

Land cover	Soil series	Particle size distribution (%)			OM	GC	$CaCO_3$	pH	EC	ρ_b	ϕ	K_{sat}	Slope	Soil structure[a]	Pore geometry[b]
		Sand	Clay	Silt	%	%	%		dS/m	kg/m^3	%	cm/h	%		
Bare (B)	Cambiorthid	48.2	8.0	43.8	0.4	2.0	32.9	7.4	1.1	1347	49.2	0.50	0–2	s	m
Alluvial (A)	Calciorthid	23.3	39.7	37.0	1.0	16.3	34.6	7.5	12.0	1400	47.2	0.47	1–3	s	f
Range (R)	Calciorthid	38.0	16.3	45.7	0.9	30.3	52.3	7.4	2.0	1317	50.3	0.76	3–5	sph	m
Trees (T)	Cambiorthid	43.7	7.1	49.2	1.6	9.7	39.8	8.0	14.6	1309	50.6	3.80	5–8	s	m

OM organic matter content, *GC* gravel content, ρ_b soil bulk density, φ total porosity, K_{sat} saturated soil hydraulic conductivity

[a] s represents subangular blocky–weak–medium structure, while sph represents spheroid–weak–fine structure

[b] m represents medium vesicular pores, while f represents fine vesicular pores

and alluvial sediments were associated by a thin surface crust that restricts the water and solute transport considerably as indicated by low K_{sat} rates of 0.5 and 0.47 cm/h for bare lands and alluvial sediments, respectively.

The existing two main soil series at the study area showed high heterogeneity as indicated by their morphological, chemical, and physical properties (Table 1). This variability might be explained by the differences in existing LULC and management practices. In general, soils of the study area are characterized by poor aggregation (i.e., low aggregate size and stability), where the average soil organic content ranged from 0.4 % for bare lands to 1.6 % for irrigated tree lands. Thus, soil bulk density ranged from 1,309 to 1,400 kg/m^3 for tree lands and bare lands, respectively.

Soil morphology

Soil morphology was effective in understanding the effect of variable combinations of gravel, OM, salt, and carbonate contents on the prediction of water and solute transport. Surface soil structure morphology varied considerably from spherical pedon with medium size vascular pore geometry to subangular blocky with vascular pore geometry ranging from fine to medium size (Table 1). The fine low-continuity pores associated with alluvial sediments restricted the water and solute transport as indicated by the lowest K_{sat} value of 0.47 cm/h, while high vascular pore sizes of high continuity under tree lands accelerated vertical water movement as indicated by a high K_{sat} value of 3.80 cm/h. Although the bare soil had similar surface structure properties as tree lands, however, the existing soil crust prohibited water infiltration dramatically as reflected by its low K_{sat} of 0.50 cm/h.

Breakthrough curve analyses

According to BTC analyses, there existed huge variations in solute transport parameters among the tested sites even under small scale (Fig. 2). Based on the figure, the time required for the effluents to reach its maximum concentration (upper

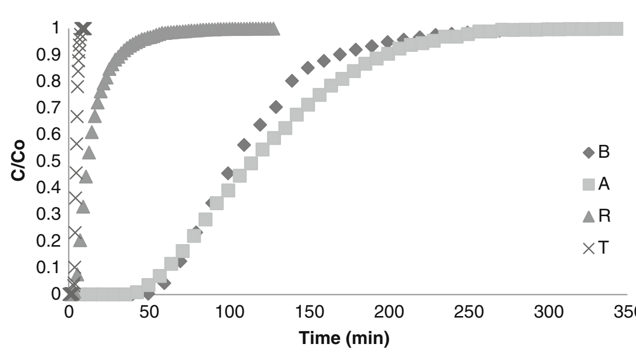

Fig. 2 BTCs for the surface vertical soil columns of the four study sites

Table 2 Solute transport parameters estimated using CDE modeling

Parameter	Land cover type			
	Bare (B)	Range (R)	Trees (T)	Alluvial (A)
Dispersion coefficient (cm^2/day)	98.02	1,339.88	329.28	52.23
Pore water velocity (m/day)	1.69	8.44	17.99	1.46
Retardation (unitless)	2.58	1.40	1.21	2.09
R^2 (%)	96	97	95	99
RMSE	0.0164	0.0120	0.0121	0.0117

boundary condition) ranged from 10 to 350 min at worse cases. The CDE analyses using JMP statistical software was able to parameterize solute transport coefficients with high accuracy as indicated by low RMSE values of less than 0.02 % (Table 2 and Fig. 3).

Pore water velocities varied from 1.46 to 17.99 m/day, while the dispersion coefficients varied from 52.23 to 1,339.88 m^2/day. The highest pore water velocity existed under tree lands (17.99 m/day) that can be explained by the associated high site slope and well developed structural system as inferred by the associated high K_{sat} value. On the other hand, the lowest pore water velocity (1.46 m/day) that existed under alluvial sediment was primarily due to both the existence of a surface crust and the soil being characterized by fine low-continuity pores.

At the same time, the highest dispersion coefficient (1,339.88 m^2/day) existed under range lands, while the lowest magnitude (52.23 m^2/day) existed under alluvial sediment. These results coincide with the morphological analyses described before. The variations in both pore water velocity and dispersion coefficient are a function of the pore geometry and tortuosity; thus, well structured pore systems favors pore water velocity while high gavel content restricts vertical movements and thus induced dispersion coefficient to its maximum.

Correlation analysis of solute transport parameters with soil properties

According to the correlation results in Table 3, it seemed that solute transport parameters were significantly ($P<0.05$) correlated to soil physical and chemical properties. Diffusion coefficient is strongly affected by gravel and $CaCO_3$ content (r^2=0.99 and 0.84, respectively), while pore water velocity is strongly correlated with silt and organic matter content (r^2=0.83 and 0.84, respectively).

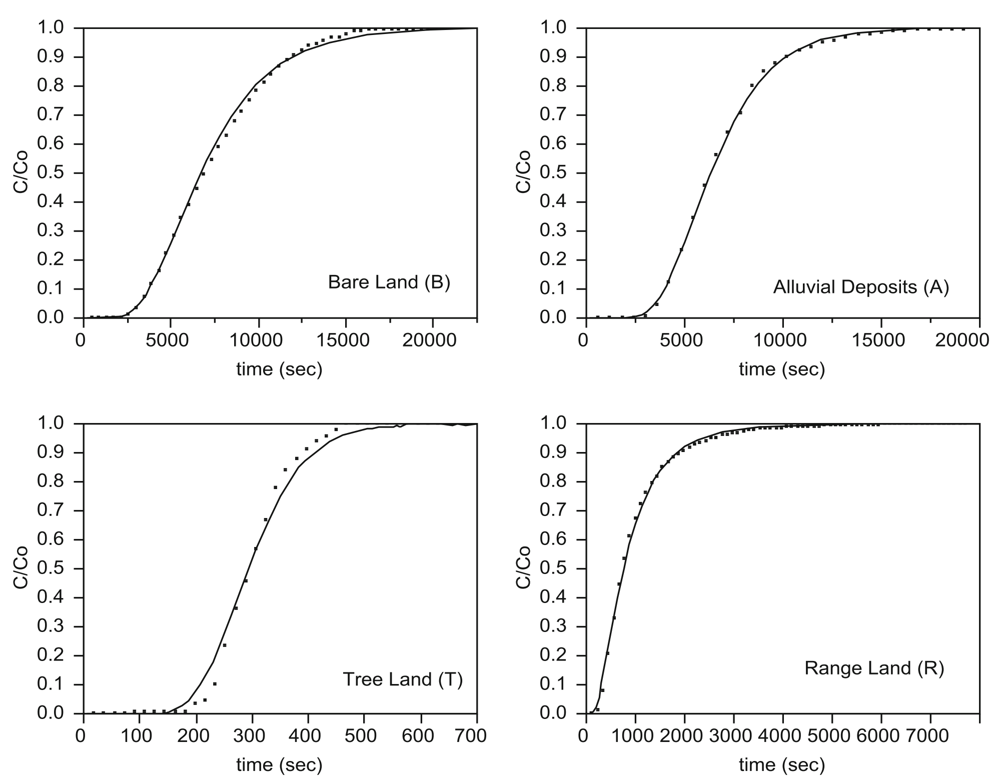

Fig. 3 CDE parameterization using JMP statistical analysis

Table 3 Correlation matrix (r) for solute transport parameters with soil physical and chemical properties

	D	V	R	Sand	Clay	Silt	OM	GC	$CaCO_3$	pH	EC	ρ_b	ϕ	K_{sat}
D	1.00	0.29	−0.59	0.08	−0.19	0.40	0.06	0.84	0.99	−0.22	−0.43	−0.58	0.58	−0.06
V		1.00	−0.87	0.35	−0.53	0.83	0.84	0.09	0.41	0.86	0.49	−0.78	0.78	0.94
R			1.00	0.01	0.20	−0.61	−0.84	−0.56	−0.72	−0.62	−0.43	0.64	−0.64	−0.69
Sand				1.00	−0.98	0.78	−0.17	−0.46	0.02	0.19	−0.41	−0.74	0.74	0.35
Clay					1.00	−0.90	−0.02	0.35	−0.16	−0.32	0.30	0.86	−0.86	−0.49
Silt						1.00	0.40	−0.04	0.44	0.56	−0.03	−0.98	0.98	0.73
OM							1.00	0.17	0.22	0.89	0.85	−0.33	0.33	0.85
GC								1.00	0.87	−0.27	−0.13	−0.13	0.13	−0.21
$CaCO_3$									1.00	−0.08	−0.27	−0.60	0.59	0.07
pH										1.00	0.80	−0.42	0.42	0.98
EC											1.00	0.16	−0.16	0.66
ρ_b												1.00	−1.00	−0.61
ϕ													1.00	0.61
K_{sat}														1.00

GC gravel content, *OM* organic matter, ρ_b soil bulk density, ϕ total porosity, K_{sat} saturated soil hydraulic conductivity

The retardation had a strongly negative correlation with $CaCO_3$ content (r^2=−0.72). It seemed that the carbonate in these soils has two opposite effects on bromide transport depending on the soil moisture condition. At unsaturated conditions, $CaCO_3$ rapidly absorbed and retained water, thus restricting the transport of water and solute within the soil system. At saturation, $CaCO_3$ function as absorbent was negligible, and thus, its physical effect as a cementing agent was more favored to produce macropore conductive flow. This result agrees with previous studies which found that the calcareous soils retained more water than noncalcareous soil at the same water potential (Hennessy et al. 1983; Duniway et al. 2007).

Also, the correlation matrix identified that the soil organic matter had a strong negative correlation (r^2=−0.84) with solute retardation indicating the importance of the direct physical effect of organic matter in enhancing soil porosity and thus solute transport rate. The effect of the positive charges of the organic matter on the retardation of bromide movement was negligible in this study due to its low quantity at arid environments.

The existing adhered gravel–soil matrix at range land acted as a barrier for vertical flow and thus increased the tortuosity of the pore system. On the other hand, the increase of organic matter favored more aggregation and thus enhanced the vertical movement of water and solute as indicated by strong positive correlation with pore water velocity.

Dye tracing

The maximum dye staining distances in both vertical and horizontal dimensions at each site are presented in Table 4. Maximum vertical dye staining depth (30 cm) was observed under tree lands followed by range lands (25 cm) then bare soil (11 cm) and alluvial sediments (10 cm). On the other hand, maximum horizontal staining was observed under range lands (20 cm) followed by tree lands (17 cm) then bare soil (13 cm) and alluvial sediments (12 cm). These results coincide with the BTC laboratorial analyses. However, the measured depth of vertical dye movement is believed to be less than expected due to the influence of carbonate content. According to Flury and Flühler (1995), retardation of Brilliant Blue FCF dye could be more obvious in calcareous soils with high percentage of $CaCO_3$ due to the formation of ion pairs between the dye and Ca^{2+}.

Dye tracing was able to indicate preferential flow paths and flow pattern at each site. Dye staining of long continuous root channels under tree land was indicative of the preferable solute conductive transport mechanism. Also, dye staining on the lateral moderate pores associated with shrub roots and the staining on the gravel surfaces prove the theory of higher diffusion rates associated with adhered gravel content under range land.

Table 4 Maximum dye staining vertical and lateral depth of Brilliant Blue FCF at each LULC type

Maximum penetrating depth (cm)	Land cover type			
	Bare (B)	Range (R)	Trees (T)	Alluvial (A)
Vertical dimension	11	25	30	10
Horizontal dimension	13	20	17	12

It was more practicable to notice the longer time period required for the dye to infiltrate through the rings at bare soil and alluvial sediment. The existing thin crust had restricted the vertical dye flow to the extent of the ring. The dye was more adsorbed within the ring zone and limited to the fine visible pores.

Summary and conclusions

Generally, arid surface soils are characterized by poor aggregation, crust formation, moderate to strong calcareous, and moderate to high saline with large gravel contents. All these combined factors may complicate the estimation of water and solute transport in these soils. BTC analyses revealed the importance of LULC effect through its direct influence on soil surface structural morphology of both pedon and pore systems.

The relatively well developed structural system under tree lands enhanced the convective solute transport. On the other hand, bare soil and alluvial sediment are weakly developed systems associated with a low-continuity porous system that favors the dispersive solute movement. The soil system under range lands is of modest case, where the soil morphological features favor the balance between convective and dispersive solute transport. Thin crust formations at alluvial sediment and bare soil restricted the water and solute transport significantly, where K_{sat} and pore water velocity ranged from 0.47 to 0.50 cm/h and 1.46 to 1.69 m/day, respectively, while high vascular pore size of high continuity under tree lands accelerated vertical water movement and thus increased K_{sat} and pore water velocity to 3.80 cm/h and 18.0 m/day, respectively.

Correlation analysis of solute transport parameters with soil physical and chemical properties was helpful in explaining the huge variability in BTC results. The solute transport in arid soil is highly affected by $CaCO_3$, gravel, and organic matter contents. Gravel and $CaCO_3$ contents were highly correlated (r=84 and 99 %, respectively) with a dispersion coefficient induced by the increase of pore system tortuosity, thus decreasing the retardation factor significantly (r=−56 and −72 %, respectively). Also, organic matter content was highly effective in enhancing soil porous conductivity, thus increasing the pore water velocity (r=84 %).

Dye tracing is an effective tool to provide evidence on water and solute transport at field scale. The dye staining was capable of showing the preferential flow paths that govern the conductive flow under tree land and the lateral dispersive flow induced by gravel content effect under range land.

Acknowledgments Great thanks to the Scientific Research Deanship at the Hashemite University for funding this project.

References

Al-Qinna M, Salahat M, Shatnawi Z (2008) Effects of carbonates and gravel contents on hydraulic properties in gravely-calcareous soils Dirasat. Agriculture Science 35:145–158

Blake GR, Hartge KH (1986) Bulk density. In: Klute A (ed) Methods of soil analysis, 2nd edn. ASA, Madison, pp 363–375

Costa JL, Prunty L (2006) Solute transport in fine sandy loam soil under different flow rates. Journal of Agricultural Water Management 83:111–118

Dousset S, Thevenot M, Pot V, Šimunek J, Andreux F (2007) Evaluating equilibrium and non-equilibrium transport of bromide and isoproturon in disturbed and undisturbed soil columns. J Contam Hydrol 94:261–276

Duniway MC, Herrick JE, Monger HC (2007) The high water-holding capacity of petrocalcic horizons. Soil Science Society of American Journal 71(3):812–819

Ersahin S, Papendick RI, Smith JL, Keller CK, Manoranjan VS (2002) Macropore transport of bromide as influenced by soil structure differences. Geoderma 108:207–223

Finke PA, Hutson JL (2008) Modelling soil genesis in calcareous loess. Geoderma 145:462–479

Flury M, Flühler H (1995) Tracer characteristics of Brilliant Blue FCF. Soil Science Society of American Journal 59:22–27

Flury M, Flühler H, Jury WA, Leuenberger J (1994) Susceptibility of soils to preferential flow of water: a field study. Water Recourse Research 30:1945–1954

Gee GW, Bauder RH (1986) Particle-size analysis. In: Klute A (ed) Methods of soil analysis, 2nd edn. ASA, Madison, pp 383–411

Ghodrati M, Jury WA (1990) A field study using dyes to characterize preferential flow of water. Soil Science Society of American Journal 54(6):1558–1563

Grossman RB, Reinsch TG (2002) Bulk density and linear extensibility. In: Dane JH, Topp GC (eds) Methods of soil analysis, 1st edn. SSSA, Madison, pp 201–228

Hennessy JT, Gibbens RP, Tromble JM, Cardenas M (1983) Water properties of caliche. J Range Manage 36(6):723–726

Jalali M, Moharrami S (2007) Competitive adsorption of trace elements in calcareous soils of western Iran. Geoderma 140:156–163

JMP (2009) Statistics and graphics guide. SAS Institute Incorporation, Cary

Jørgensen PR, Helstrup T, Urup J, Seifert D (2004) Modeling of nonreactive solute transport in fractured clayey till during variable flow rate and time. J Contam Hydrol 68:193–216

Klute A (1986) Water retention: laboratory methods. In: Klute A (ed) Methods of soil analysis, 2nd edn. ASA, Madison, pp 635–662

Klute A, Dirksen C (1986) Hydraulic conductivity and diffusivity: laboratory methods. In: Klute A (ed) Methods of soil analysis, 2nd edn. ASA, Madison, pp 687–734

Larsbo M, Jarvis N (2005) Simulating solute transport in a structured field soil: uncertainty in parameter identification and predictions. J Environ Qual 34:621–634

Leij FJ, van Genuchten MT (1995) Approximate analytical solutions for solute transport in two-layer porous media. Transport in Porous Media 18:65–85

Li Z, Hong H (2009) Retardation of chromate through packed columns of surfactant-modified zeolite. J Hazard Mater 162:1487–1493

Loeppert RH, Suarez DL (1996) Carbonate and gypsum. In: Sparks DL (ed) Methods of soil analysis, 3rd edn. SSSA, Madison, pp 437–474

Ministry of Agriculture (1994) National soil map and landuse. Hunting Technical Services Ltd and Soil Survey and Land Research Centre, Amman

Mojid MA, Vereecken H (2005) On the physical meaning of retardation factor and velocity of a nonlinearly sorbing solute. J Hydrol 302:127–136

Nelson DW, Sommers LE (1996) Total carbon, organic carbon, and organic matter. In: Sparks DL (ed) Methods of soil analysis, 3rd edn. SSSA, Madison, pp 961–1010

Rhoades JD (1996) Salinity: electrical conductivity and total dissolved solids. In: Sparks DL (ed) Methods of soil analysis, 3rd edn. SSSA, Madison, pp pp. 417–436

Samsoe-Petersen L, Larsen EH, Larsen PB, Bruun P (2002) Uptake of trace elements and PAHs by fruit and vegetable from contaminated soils. J Environ Sci Technol 36:3057–3063

Scott HD (2000) Soil physics: agricultural and environmental applications. Iowa State University Press, Ames

Thomas GW (1996) Soil pH and soil acidity. In: Sparks DL (ed) Methods of soil analysis, 3rd edn. SSSA, Madison, pp 475–490

van Genuchten MTh, Alves WJ (1982) Analytical solutions of the one-dimensional convective–dispersive solute transport. USDA Tech. Bull. No. 1661. Washington, D.C.

Vogeler I, Horn R, Wetzel H, Krümmelbein J (2006) Tillage effects on soil strength and solute transport. Journal of Soil and Tillage Research 88:193–204

Wong DWS, Lee J (2005) Statistical analysis of geographic information with ArcView GIS and ArcGIS. Wiley, USA

Yolcubal I, Akyol NH (2008) Adsorption and transport of arsenate in carbonate-rich soils: coupled effects of nonlinear and rate-limited sorption. Journal of Chemosphere 73:1300–1307